Experimental demonstration of multi-Gbps multi sub-bands FBMC transmission in mm-wave radio over a fiber system

HUM NATH PARAJULI,[1,*] HAYMEN SHAMS,[2] LUIS GUERRERO GONZALEZ, [2] ESZTER UDVARY,[1] CYRIL RENAUD, [2] AND JOHN MITCHELL[2]

[1]Department of Broadband Info-Communication and Electromagnetic Theory, Budapest University of Technology and Economics, Egri Jozsef utca, 18, 1111, Budapest, Hungary
[2]Department of Electronic and Electrical Engineering, University College London (UCL), Torrington Place, WC1E 7JE, London, UK
*hum.nath.parajuli@hvt.bme.hu

Abstract: The filter bank multicarrier (FBMC) modulation format is considered as a potential candidate for future wireless 5G due to its feature of high suppression for out-of-band emissions, which allows combining multiple sub-bands with very narrow band-gaps, and hence increases the overall wireless transmission capacity. In this paper, we experimentally demonstrate the generation of multi sub-bands FBMC signals at millimeter-wave (mm-wave) for radio-over-fiber (RoF) systems. The designed multi sub-bands FBMC system consists of 5 sub-bands of 800 MHz with inter sub-band gaps of 781.25 kHz. The composite 5 sub-bands FBMC signal is generated with no band-gap between dc to the first sub-band to preserve the bandwidth of the system. Each FBMC sub-band consists of 1024 sub-carriers and is modulated with uncorrelated data sequences. The aggregate FBMC signal is carried optically by externally modulating a free running laser and is converted to millimeter waves (mm-waves) by photomixing with another free running laser at a frequency offset of 53 GHz. At the receiver, the received electrical mm-wave signal is down-converted to an intermediate frequency (IF) and then post-processed using digital signal processing (DSP) techniques. With the use of the simple recursive least square (RLS) equalizer in the DSP receiver, the achieved aggregate data rate is 8 Gbps and 12 Gbps for 16 quadrature amplitude modulation (QAM), and 64 QAM, respectively with a total bandwidth of 4.2 GHz. The system performance is evaluated by measuring error vector magnitude (EVM) and bit error rate (BER) calculations.

References and links

1. T. S. Rappaport, S. Sun, R. Mayzus, H. Zhao, Y. Azar, K. Wang, G. N. Wong, J. K. Schulz, M. Samimi, and F. Gutierrez, "Millimeter wave mobile communications for 5G cellular: it will work!" IEEE Access **1**, 335–349 (2013).
2. L. Wei, R. Q. Hu, Y. Qian, and G. Wu, "Key elements to enable millimeter wave communications for 5G wireless systems," IEEE Wirel. Commun. **21**(6), 136–143 (2014).
3. D. Novak, R. B. Waterhouse, A. Nirmalathas, C. Lim, P. A. Gamage, T. R. Clark, M. L. Dennis, and J. A. Nanzer, "Radio-over-fiber technologies for emerging wireless systems," IEEE J. Quantum Electron. **52**(1), 1–11 (2016).
4. E. P. Martin, T. Shao, V. Vujicic, P. M. Anandarajah, C. Browning, R. Llorente, and L. P. Barry, "25-Gb/s OFDM 60-GHz radio over fiber system based on a gain switched laser," J. Lightwave Technol. **33**(8), 1635–1643 (2015).
5. T. T. Nguyen, S. T. Le, Q. He, L. V. Compernolle, M. Wuilpart, and P. Mégret, "Multicarrier approaches for high-baudrate optical-fiber transmission systems with a single coherent receiver," IEEE Photonics J. **9**(2), 1–10 (2017).
6. P. Banelli, S. Buzzi, G. Colavolpe, A. Modenini, F. Rusek, and A. Ugolini, "Modulation formats and waveforms for 5G networks: who will be the heir of OFDM? An overview of alternative modulation schemes for improved spectral efficiency," IEEE Signal Process. Mag. **31**(6), 80–93 (2014).

7. J. Zhang, M. Xu, J. Wang, F. Lu, L. Cheng, H. Cho, K. Ying, J. Yu, and G. K. Chang, "Full-duplex quasi-gapless carrier aggregation using FBMC in centralized radio-over-fiber heterogeneous networks," J. Lightwave Technol. **35**(4), 989–996 (2017).
8. M. Xu, J. Zhang, F. Lu, J. Wang, L. Cheng, H. J. Cho, M. I. Khalil, D. Guidotti, and G. K. Chang, "FBMC in next-generation mobile fronthaul networks with centralized pre-equalization," IEEE Photonics Technol. Lett. **28**(18), 1912–1915 (2016).
9. A. Saljoghei, F. A. Gutiérrez, P. Perry, D. Venkitesh, R. D. Koipillai, and L. P. Barry, "Experimental comparison of FBMC and OFDM for multiple access uplink PON," J. Lightwave Technol. **35**(9), 1595–1604 (2017).
10. S. Y. Jung, S. M. Jung, and S. K. Han, "AMO-FBMC for asynchronous heterogeneous signal integrated optical transmission," IEEE Photonics Technol. Lett. **27**(2), 133–136 (2015).
11. Y. T. Hsueh, C. Liu, S. H. Fan, J. Yu, and G. K. Chang, "A novel full-duplex testbed demonstration of converged all-band 60-GHz radio-over-fiber access architecture," *OFC/NFOEC)*, (Optical Society of America, 2012), pp. 1–3, paper OTu2H.5.
12. M. Zhu, A. Yi, Y. T. Hsueh, C. Liu, J. Wang, S. C. Shin, J. Yu, and G. K. Chang, "Demonstration of 4-band millimeter-wave radio-over-fiber system for multi-service wireless access networks," *2013 Optical Fiber Communication Conference and Exposition and the National Fiber Optic Engineers Conference (OFC/NFOEC)*, (Optical Society of America, 2013), pp. 1–3, paper OM3D.4.
13. R. P. Giddings, E. Hugues-Salas, and J. M. Tang, "30Gb/s real-time triple sub-band OFDM transceivers for future PONs beyond 10Gb/s/λ," *39th European Conference and Exhibition on Optical Communication (ECOC 2013)*, London, 2013, pp. 1–3.
14. H. Shams, M. J. Fice, L. Gonzalez-Guerrero, C. C. Renaud, F. van Dijk, and A. J. Seeds, "Sub-THz wireless over fiber for frequency band 220–280 GHz," J. Lightwave Technol. **34**(20), 4786–4793 (2016).
15. K. Werfli, P. A. Haigh, Z. Ghassemlooy, N. B. Hassan, and S. Zvanovec, "A new concept of multi-band carrier-less amplitude and phase modulation for bandlimited visible light communications," *2016 10th International Symposium on Communication Systems, Networks and Digital Signal Processing (CSNDSP)*, 2016, pp. 1–5.
16. Project Document "FBMC physical layer: a primer," (PHYDYAS, Jan. 2010). [Online available: http://www.ict-phydyas.org/]
17. ETSI, "LTE; Evolved universal terrestrial radio access (E-UTRA); Base station (BS) radio transmission and reception", 2015.
18. Z. Li, M. S. Erkılınç, K. Shi, E. Sillekens, L. Galdnio, B. C. Thomsen, P. Bayvel, and R. I. Killey, "SSBI mitigation and the Kramers–Kronig scheme in single-sideband direct-detection transmission with receiver-based electronic dispersion compensation," J. Lightwave Technol. **35**(10), 1887–1893 (2017).

1. Introduction

The frequency bands at higher carrier frequencies such as millimeter-wave (mm-wave) are considered as an alternative solution to overcome the problem of frequency congestion of the current wireless transmission system. Future wireless 5G networks are expected to provide 1-10 Gbps wireless access to the end users [1–3]. The multicarrier system is a potential solution to increase the spectral efficiency in future radio over fiber (RoF) systems. One of the heavily studied modulation format in multicarrier system is orthogonal frequency division multiplexing (OFDM) because of its merits of better spectral efficiency and robustness to the linear optical impairments such as chromatic dispersion (CD) [4]. However, OFDM modulation requires cyclic prefix (CP) in the overhead to reduce the inter symbol interference (ISI) and inter carrier interference (ICI), which reduces the spectral efficiency. Moreover, the large out of band emission of the OFDM subcarriers requires large guard bands in the multi sub-bands system. These problems can be overcome through filter bank multicarrier (FBMC) system [5, 6]. The side lobe suppression of FBMC is about 40 dB in comparison with OFDM which is only about 13 dB [7]. Furthermore, FBMC does not need to include CP for each symbol due to the combining features of FBMC prototype filters and the use of offset quadrature amplitude modulation (OQAM) scheme. In consequence, this leads to increase the bandwidth efficiency and enables the asynchronous carrier aggregation [5–8].

FBMC based passive optical network (PON) was experimentally demonstrated in [9]. The performance comparison of OFDM and FBMC carrier aggregated signals at mm-wave frequencies was recently studied with the aggregated bandwidth of less than 1.5 GHz [7, 8]. These demonstrations show that the FBMC outperforms the OFDM for equivalent design parameters. Adaptively modulated FBMC was also demonstrated in the wired-wireless converged network with the aggregated bandwidth of 1.5 GHz [10]. The future 5G RoF systems should be capable of supporting multi sub-bands and multi services in radio signals

to keep the compatibility with the current legacy wireless services [11–15]. All of the above mentioned demonstrations of FBMC based multiple sub-band signals for mm-wave transmission are dealt with sub-band bandwidth of less than 220 MHz and aggregate bandwidth of less than 1.5 GHz, and hence low overall data rate. In this paper, we experimentally demonstrate 5 FBMC sub-bands of 800 MHz with an aggregate bandwidth of 4.2 GHz at mm-wave in a RoF system. The signal with 5 FBMC sub-bands is generated with no bandgap between dc to first sub-band which preserves the bandwidth of the system. Each FBMC sub-band signal is fed with uncorrelated data sequences and separated with a narrow bandgap of 781.25 kHz between the sub-bands. At the receiver, the FBMC sub-bands are extracted and demodulated by using digital signal processing (DSP) techniques. The aggregate data rate of 8 Gbps and 12 Gbps is achieved with 16 QAM, and 64 QAM, respectively. The performance is optimized with the use of recursive least square (RLS) equalizer.

The rest of the paper is organized as follows. In section 2, the description of the FBMC multi-sub-bands signal generation method is given. In section 3, the implemented system model of optical transmission setup is described. Section 4 presents the signal processing methods for received mm-wave multi-sub-band FBMC signal extraction and demodulation. Section 5 illustrates the experimental results and discussion of the multi sub-band FBMC signals performance. Finally, section 6 concludes the paper.

2. Multi-sub-bands FBMC signal generation

In the FBMC system, a set of parallel symbols are transmitted through a bank of modulated filters, called synthesis filter bank (SFB) and in the receiving side the data symbols are recovered through a bank of matched modulated filters called analysis filter bank (AFB). Each filter in SFB and AFB is based on the specially designed prototype filter. The structure of OFDM and FBMC are similar but the differences lie in the choice of prototype filter and the choice of symbol time spacing. In OFDM, prototype filter is a rectangular window with the amplitude of 1 which results in large magnitude sidelobes but in the case of FBMC, it is specially designed to reduce the sidelobes in large extent. In FBMC system, the duration of prototype filter is chosen to be integer multiples of symbol time spacing, which causes successive symbols overlapping. To maintain the orthogonality the concept of OQAM can be used. OQAM modulation can be realized from QAM modulation by making the adjacent symbols delayed with half symbol period offset [5, 16].

Figure 1(a) shows the simplified DSP block diagram for generating a single sub-band FBMC signal. The MATLAB routines are developed to generate offline code for a single sub-band FBMC signal [7, 16]. First, the input data stream is mapped into M-QAM format, and then it is converted from serial to parallel (S/P) streams. Then, the QAM symbols are converted into OQAM symbols by making the adjacent symbols delayed with half symbol period offset. After this, the inverse fast Fourier transform (IFFT) is applied to convert the OQAM symbols into time domain symbols. In our design, each subcarrier is filtered with a well-designed prototype filter with 4-tap length that can suppress the subcarrier side lobes around 40 dB, called synthesis polyphase filtering (SPF) [16]. After the parallel to serial (P/S) conversion process, root raised cosine (RRC) filter with a roll off factor of 0.3 is applied to optimize the signal to noise ratio (SNR). Then, the baseband FBMC signal is digitally upconverted to a selected sub-band intermediate frequency (IF). The same process is applied for all other FBMC sub-bands, and then combined together to generate a composite signal of 5 FBMC sub-bands as shown in Fig. 1(b). After this, normalization and clipping are applied to maintain the peak-to-peak voltage amplitude at 500 mV. Thus, the generated code output is uploaded into an arbitrary waveform generator (AWG).
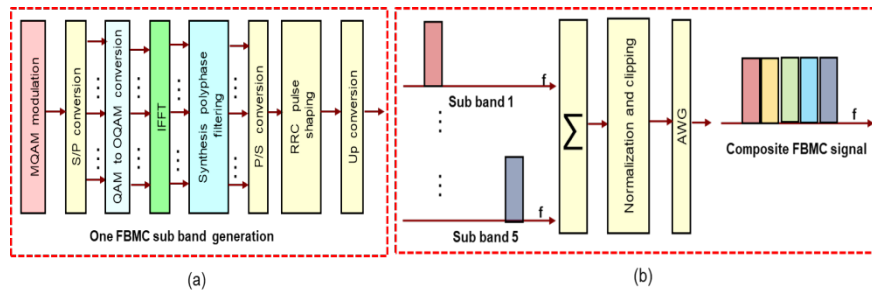
Fig. 1. Functional block diagram of (a) a single FBMC signal generation, and (b) composite FBMC signal of 5 sub-bands.

The designed parameters for the multi sub-band FBMC signals are given in Table 1. The sampling frequency is 40 GS/s and each OQAM symbol is up sampled with 50 samples. The size of IFFT/FFT is 1024. Each FBMC sub-band has a bandwidth of 800 MHz. The total bandwidth of the composite 5 sub-band FBMC signals is about 4.0031 GHz with an inter sub-bandgap of 781.25 kHz. Due to the RRC roll-off factor of 0.3, the bandwidth broadens to 4.2431 GHz. Figure 2 shows offline generated composite 5 sub-band FBMC signals with bandwidth assignments for each sub-band. The FBMC sub-bands are digitally up-converted to 520 MHz, 1.3208 GHz, 2.1216 GHz, 2.9293 GHz and 3.723 GHz. The time window of a single sub-band and 5 sub-bands signal is identical and equal to 12.8 µs. For the 16 QAM case, 102,400 bits are used and for 64 QAM case 153,600 bits are used.
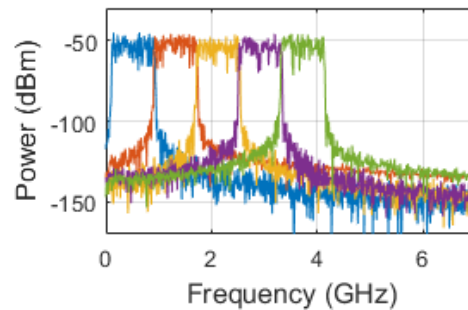

Fig. 2. Electrical spectrum of offline generated 5 sub-bands FBMC signal.

Table 1. Design parameters of multi sub-band FBMC signal generation

Parameters	Values		Parameters	Values
Modulation format	16QAM	64QAM	Sub-bands spacing	781.25 kHz
No. of bits	102400	153600	One sub-band BW	800 MHz
Bit rate	8 Gbps	12 Gbps	Multi sub-bands BW	4.2431 GHz
Sampling frequency	40 GS/s		Time window	12.8 µs
No of sub-bands	5		RRC roll off	0.3

3. Experimental setup

Figure 3 represents the simplified block diagram of the optical transmitter and receiver at the back-to-back configuration. In the optical transmitter, a distributed feedback (DFB) laser at 1553.73 nm wavelength with a linewidth of 10 kHz is used to feed the intensity modulator (IM). The IM is a chirp-less modulator with half wave voltage of 7.0 V and biased at the quadrature point. The IM is driven by an amplified 5 FBMC sub-bands signal generated from AWG channel. The peak-to-peak amplitude from AWG is 500 mV, and the sampling rate is 40 GS/s. Then, it is amplified with radio frequency (RF) amplifier to 4.4 V before applying to IM. The modulated optical signal is then optically amplified by erbium doped fiber amplifier

(EDFA) and filtered by 1 nm optical band pass filter (OBPF) to remove the amplified spontaneous emission (ASE) noise. After that, the amplified optical signal is coupled with a free running external cavity laser (ECL) using a 3 dB coupler. The optical spectrum of the generated signal is given in Fig. 3 as an inset figure. The separation of the two free running lasers is adjusted to be 53 GHz by tuning the ECL wavelength to a wavelength of 1553.30 nm. In the optical receiver, the combined optical signal is converted to mm-wave at 53 GHz by fast photodiode of 70 GHz bandwidth. The generated RF signal is then mixed with an electrical LO at 41.5 GHz to down-convert it to an intermediate frequency (IF) at 11.5 GHz. The received IF signal is amplified by an RF amplifier, and then recorded with the real-time scope (RTS) for further offline DSP using the developed MATLAB code.
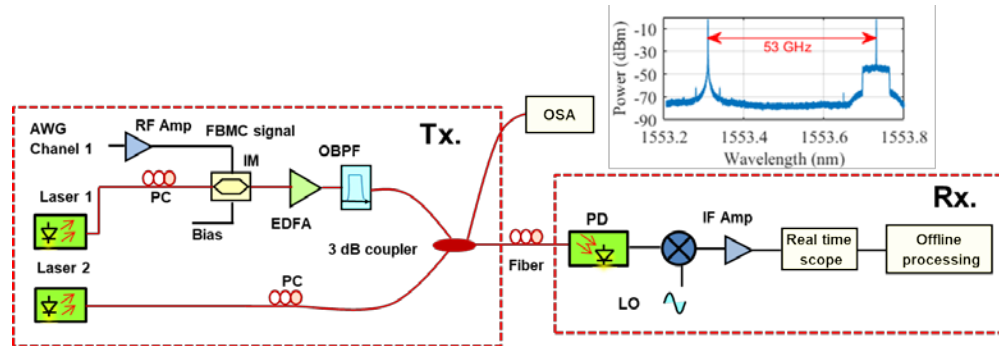

Fig. 3. Experimental setup for multi FBMC sub-bands transmitter and receiver. The inset figure is the optical spectrum of the mixed optical signals at the OSA.

4. DSP receiver offline processing

Figure 4 represents the simplified block diagram of the applied DSP at the receiver. The received IF signal is captured at 40 GS/s from the real-time scope, and the spectrum of the received signal is shown in Fig. 5(a). First, the IF signal is filtered by square bandpass filter which extracts the two sidebands of the received signal as shown in Fig. 5(b). The signal is then digitally down converted to the baseband signal by using an envelope detector as shown in Fig. 5(c). After low pass filter, the signal spectrum is obtained as shown in Fig. 5(d).
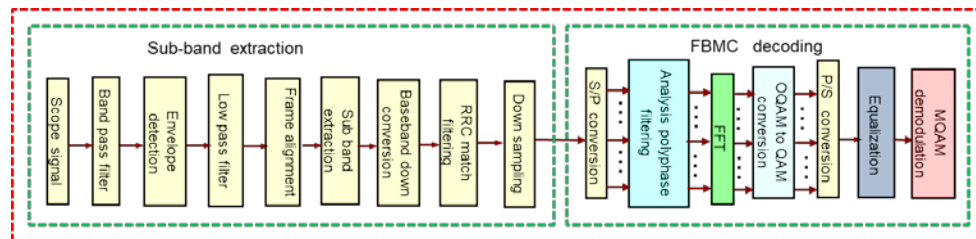

Fig. 4. Digital signal processing to recover and demodulate the received multi sub-band FBMC signals.

The transmitter and receiver symbol alignment is achieved with the cross-correlation technique. Each FBMC sub-band is extracted by down-converting it with its corresponding IF frequency used in the signal generation, and then RRC low pass filtering is applied. The produced signal is resampled at 2 samples per OQAM symbol. The FBMC decoding routines are applied as shown in Fig. 4 [7, 16]. First, the serial sample points are converted into parallel stream. After this, the same prototype filter as used in FBMC coding side is applied in each subcarrier, called analysis poly-phase filtering (APF). Consequently, FFT, OQAM to QAM conversion, and P/S conversion processes are performed. The first 16 QAM samples from each sub-band are used as a training signal to calculate the channel response which is

used to equalize the signal. Furthermore, a simple 1 tap recursive least square (RLS) equalizer with forgetting factor of 0.92 is employed to optimize the equalization process. Then, the performance of the signal is evaluated with EVM and BER calculations.
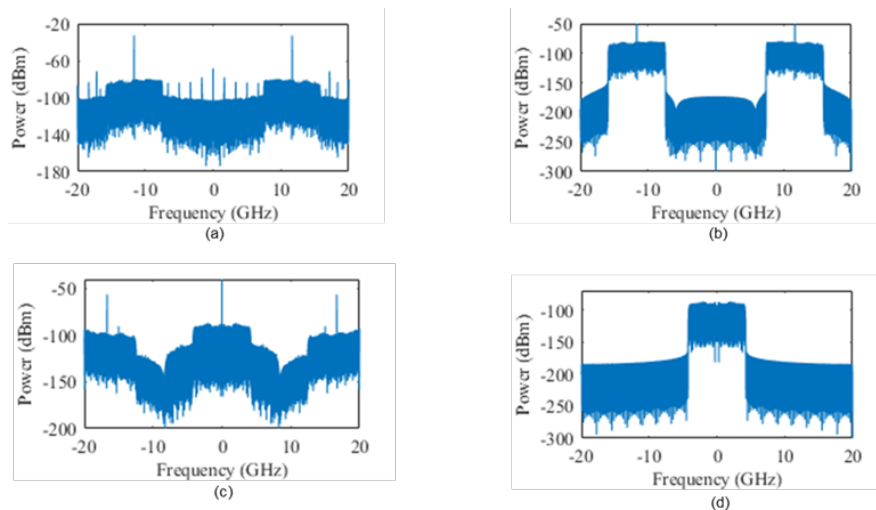

Fig. 5. Electrical spectra of the received composite 5 FBMC sub-bands signal after (a) IF amplifier, (b) bandpass filter, (c) envelope detector, and (d) low pass filter.

5. Results and discussions

Figure 6(a) represents the calculated error vector magnitude (EVM) values of 16 QAM (8 Gbps) and 64 QAM (12 Gbps) of the composite 5 sub-bands FBMC signal in terms of the received optical power. Figure 6(b) represents the corresponding bit error rate (BER) values at the same received optical power. As shown in Fig. 6(a), for the case of 64 QAM modulation order, EVM values are slightly higher in comparison with 16 QAM modulation order. For the received optical power of 2.5 dBm, the BER of 16 QAM is 8×10^{-5} and 64 QAM is 4×10^{-3}. The constellation diagrams at the received optical power of 2.5 dBm for both 16 QAM and 64 QAM cases are also shown as insets in Fig. 6(b). This experiment achieved EVM below 12.5% for 16 QAM and 8% for 64 QAM as a figure of merit as proposed by 3GPP LTE [17]. These limits were achieved for received optical power of −1.5 dBm and 2.5 dBm for 16 QAM and 64 QAM, respectively.
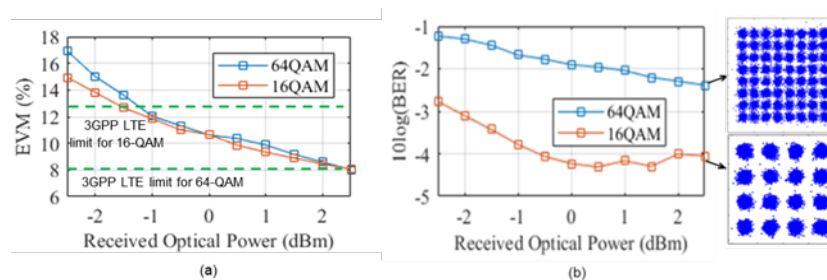

Fig. 6. (a) EVM and (b) BER performances versus ROP for 5 sub-bands FBMC signal. Inset figures are the constellations of 16QAM and 64QAM for ROP of 2.5 dBm.

Figures 7(a) and 7(b) represent the calculated error vector magnitude (EVM) values of 16 QAM (8 Gbps) and 64 QAM (12 Gbps) cases for each sub-bands at different received optical powers. The obtained results were measured without the baseband gap between the dc to the first sub-band to preserve the bandwidth efficiency of the system. Due to the square law

envelope detection process the signal to signal beating interference (SSBI) occurs. The SSBI term appears adjacent to the dc and interferes with the low frequency signal term close to dc. To avoid the effect of SSBI, it is required to keep certain frequency gap between dc to first sub-band but this reduces the bandwidth efficiency. Another approach is to use SSBI mitigation using DSP techniques that can improve the system performance as well as preserve the bandwidth of the system [18]. Without using SSBI mitigation techniques, the BER in the order of 10^{-3} for 12 Gbps data rate and in the order of 10^{-5} for 8 Gbps data rate were achieved at the bandwidth of 4.2 GHz.

Results show that to achieve the 3GPP LTE EVM percentage limit for the case of 8 Gbps, −1.5 dBm of received optical power is required and for the case of 12 Gbps, 2.5 dBm is required. In this setup, we used a mixer and an RF amplifier at the IF frequency which reduce the SNR of the received signal.
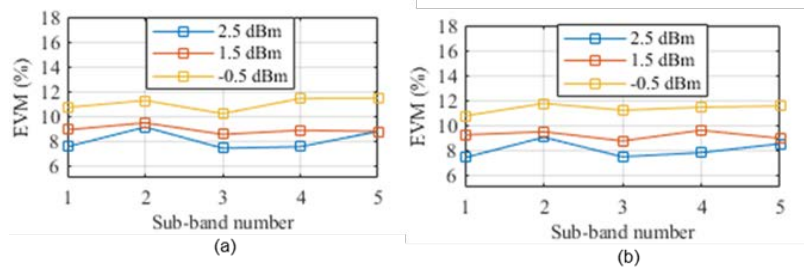

Fig. 7. EVM performances of each sub-band FBMC signal for (a) 16 QAM (b) 64 QAM.

The presented results are achieved with the addition of the simple RLS based post equalizer in the receiver DSP. Chromatic dispersion and attenuation are the major impairments for transmitting wireless signal through the fiber. In this experiment, the FBMC signal has been modulated only to one of the optical carrier and photo-mixed with unmodulated optical carrier spaced by 53 GHz. In this setup, the received signal power fading effect will be very low or negligible since power fading effect occurs only to the RF FBMC signal which is less than 5 GHz. The first null power point of the 5 GHz RF signal, with 18 ps/nm/km dispersion and 1553 nm laser wavelength occurs at 138 km. If we consider the fiber loss of 0.2 dB/km and 15 km fiber length, there will be very negligible power fading effect due to CD but the optical power loss will be 3 dB. In this case, the signal with 16-QAM (8 Gbps) data rate, at the fiber length of 15 km can be used by fulfilling the requirement of 3GPP LTE EVM percentage limit.

6. Conclusions

In this paper, we experimentally demonstrated 5 FBMC sub-bands signal of 800 MHz bandwidth per FBMC sub-band and total bandwidth of 4.2 GHz at the data rate of 8 Gbps and 12 Gbps in the radio over fiber system. The composite 5 FBMC sub-bands signal was designed without bandgap between the dc to the first sub-band to preserve the bandwidth of the system. The BER values of 8×10^{-5} for 8 Gbps case using 16 QAM and 4×10^{-3} for 12 Gbps case using 64QAM are achieved for the received optical power of 2.5 dBm. Due to the high suppression of out-of-band emission, we believe that the aggregated FBMC sub-bands will meet the expectation for the future 5G wireless with high data rate transmission for multi-user, and multi-bands wireless services feasibility.

Funding